Cancer Biology & Therapy
Publication details, including instructions for authors and subscription information:
http://www.tandfonline.com/loi/kcbt20

Discovery of a novel quinoxalinhydrazide with a broad-spectrum anticancer activity

Carmen Plasencia, Fedora Grande, Takashi Oshima, Xuefei Cao, Roppei Yamada, Tino Sanchez, Francesca Aiello, Antonio Garofalo & Nouri Neamati

Published online: 01 Mar 2009.

To cite this article: Carmen Plasencia, Fedora Grande, Takashi Oshima, Xuefei Cao, Roppei Yamada, Tino Sanchez, Francesca Aiello, Antonio Garofalo & Nouri Neamati (2009) Discovery of a novel quinoxalinhydrazide with a broad-spectrum anticancer activity, Cancer Biology & Therapy, 8:5, 458-465, DOI: 10.4161/cbt.8.5.7741

To link to this article: http://dx.doi.org/10.4161/cbt.8.5.7741

[Cancer Biology & Therapy 8:5, 1-8; 1 March 2009]; ©2009 Landes Bioscience

Research Paper

Discovery of a novel quinoxalinhydrazide with a broad-spectrum anticancer activity

Carmen Plasencia,[1] Fedora Grande,[1,2] Takashi Oshima,[1] Xuefei Cao,[1] Roppei Yamada,[1] Tino Sanchez,[1] Francesca Aiello,[1,2] Antonio Garofalo[2,*] and Nouri Neamati[1,*]

[1]Department of Pharmacology and Pharmaceutical Sciences; School of Pharmacy; University of Southern California; Los Angeles, California USA; and [2]Dipartimento di Scienze Farmaceutiche; Università della Calabria; Arcavacata di Rende (Cs), Italy

Key words: quinoxalinhydrazide, anticancer activity, preclinical evaluations, apoptosis, novel agents, xenograft studies

Previously, we discovered a novel class of salicylhydrazide compounds with remarkable activity in hormone-dependent and -independent human cancer cells. We then designed and synthesized numerous analogues. Among these analogues, a quinoxalinhydrazide compound, SC144, exhibited desirable physicochemical and drug-like properties and therefore, was selected for further preclinical investigation. In the present study, we evaluated the in vitro activity of SC144 in a range of drug-sensitive and -resistant cancer cell lines as well as its in vivo efficacy in MDA-MB-435 and HT29 mice xenograft models. The broad-spectrum cytotoxicity of SC144 is especially highlighted by its potency in ovarian cancer cells resistant to cisplatin, breast-cancer cells resistant to doxorubicin, and colon cancer cells resistant to oxaliplatin. Furthermore, its activity was independent of p53, HER-2, estrogen and androgen receptor expressions. We also examined the effect of SC144 on cell cycle progression and apoptosis in select cell lines. Considering its cytotoxicity profile in a variety of in vitro and in vivo cancer models as well as its effects on cell cycle regulation and apoptosis, SC144 appears to represent a promising agent for further clinical development.

Introduction

Traditionally, most small molecule anticancer drugs were discovered by high throughput screening (HTS) with cytotoxicity as the end-point measurement.[1] In general, most, if not all, of these drugs have multiple mechanisms of action and hence multiple mechanisms of resistance.[2] With few exceptions, their mechanisms are usually identified much later than their discovery. And the actual mechanisms of certain drugs were often found to be different than what had been originally anticipated. Although various strategies have been used to identify drug targets, it is becoming appreciated that there are no easy and straightforward ways to do so with current technologies. Two reasons can be presented to explain this. The first has to do with the intrinsic physicochemical natures of small molecule drugs (e.g., membrane permeability in many cell types) coupled with their lack of selectivity and specificity as compared to, for example, antibody-antigen recognition. Second, there is an overwhelming amount of redundancy, resulted from sequence and structural homology, built into biological systems serving as targets. This might explain why in many cases messy cytotoxic drugs, despite their off-target effects, work just as well or better than targeted therapeutics. Whatever the mechanism is, the initial and critical step in any drug discovery program is lead identification.

All 26 FDA approved drugs for HIV-1 infection are used in various combinations. By contrast, of over 100 FDA approved anticancer drugs, fewer than 25 are widely used due to their lack of drug-like properties.[3] Drug-like properties usually refer to favorable absorption and bioavailability features that a drug must have to succeed in human clinical trials. Although some drugs can be rescued by proper formulation, in most cases, a bad drug is destined to fail. Therefore, prior to lead optimization, we always carry out extensive in silico- and knowledge-based ADMET calculations to address the possible problematic properties of our novel compounds. It is also important to note that even with the best in vitro and in silico predictive models, it is still very difficult to correctly envisage drug failures due to pharmacogenomics reasons and adverse physiological responses such as QT prolongation.[4-8]

For targeted cancer therapeutics, identification of lead compounds with novel mechanisms of action, lower toxicity and enhanced activity profiles is of paramount importance.[9] Using pharmacophore models to distinguish antiviral compounds from anticancer compounds, we successfully identified a new class of leads with remarkable activity both in vitro and in vivo. Two members of these new compounds, SC21 and SC23, were previously evaluated against a range of human tumor derived cancer cell lines.[10] In an effort to optimize the physicochemical properties of these novel cytotoxic compounds, we have synthesized numerous analogues and selected SC144 for further development based on its desirable ADMET profiles. In the present study, we provided evidence that SC144 is a novel potent agent with broad-spectrum cytotoxic activities in a number of tumor cells with different characteristics. We also reported the effects of SC144 on cell

*Correspondence to: Antonio Garofalo; Dipartimento di Scienze Farmaceutiche; Università della Calabria; Arcavacata di Rende (Cs) 87036 Italy; Tel.: +39.0984.493118; Email: garofalo@unical.it/ Nouri Neamati; Department of Pharmacology and Pharmaceutical Sciences; School of Pharmacy; University of Southern California; 1985 Zonal Ave.; Los Angeles, California 90033 USA; Tel.: 323.442.2341; Fax: 323.442.1390; Email: neamati@usc.edu

Submitted: 12/19/08; Accepted: 12/31/08

Previously published online as a *Cancer Biology & Therapy* E-publication: http://www.landesbioscience.com/journals/cbt/article/7741

cycle regulation and apoptosis. Finally, we evaluated its in vivo efficacy in both breast cancer and colon cancer mice xenograft models.

Results

Chemistry. Previously, we reported on the discovery of a novel class of compounds with remarkable potency in a broad panel of cell lines. Two members of these compounds, SC21 and SC23, were further evaluated against a battery of hormone-receptor positive and negative cell lines and showed excellent in vitro and in vivo efficacy in human cancer models.[10] Encouraged by these results, we designed and built a large library of analogues. After in silico calculation of a host of parameters, including physicochemical, pharmacokinetics and drug-like properties for oral absorption, using ADMET Predictor software package (Simulations Plus, Inc., Lancaster, CA), we synthesized several closely related analogues with desirable ADMET properties for our initial studies on structure-activity relationships (SAR).[11] Among these analogues, SC144 showed excellent potency in many human cancer cell lines and, therefore, was selected for in-depth preclinical studies.

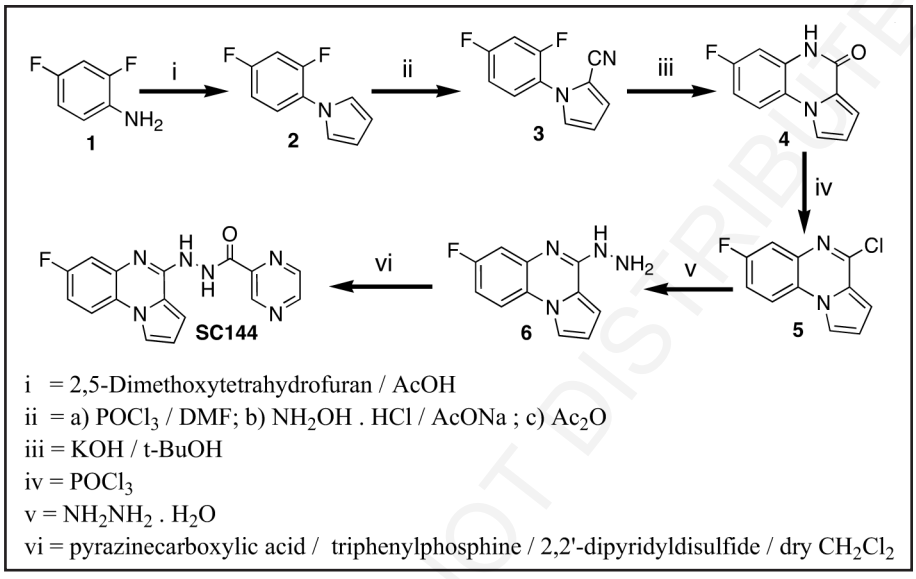

Scheme 1. Synthesis of SC144.

The synthesis of SC144 was accomplished by using commercially available 2,4-difluoroaniline, bearing a fluorine atom at position 2 as leaving group, as starting material. This was subjected to Clauson-Kaas reaction with 2,5-dimetoxytetrahydofuran to give 1-(2,4-difluorophenyl)-1*H*-pyrrole, which was transformed into the corresponding 2-carbonitrile by a one-pot modified Vilsmeier-Haack reaction.[12] The nitrile was directly cyclised to 7-fluoropyrrolo[1,2-a] quinoxalin-4(5H)-one by potassium hydroxide in *tert*-butanol. The lactam obtained was subsequently transformed into 4-chloro-7-fluoro-1H-pyrrolo[1,2-a]quinoxaline by treatment with phosphoryl chloride. This chloro derivative was then converted into the desired 1-(7-fluoro-1H-pyrrolo[1,2-a]quinoxalin-4-yl)hydrazine, which was reacted with pyrazinecarboxylic acid in the presence of triphenylphosphine and 2,2'-dipyridyldisulfide to give the expected N'-(7-fluoroH-pyrrolo[1,2-a]quinoxalin-4-yl)pyrazine-2-carbohydrazide (SC144) (Scheme 1).

SC144 shows excellent potency against a panel of human cancer cell lines. The sensitivity of a panel of 14 human cancer cell lines to SC144 was assessed by MTT assay. SC144 showed excellent activity in these cancer cell lines from different tumor origins, with IC_{50} values range from 0.14 to 4.0 μM (Table 1). The sensitivity towards SC144 was time- (data not shown) and dose-dependent (Fig. 1). Thus, the in vitro cell death increased with increasing concentrations and exposure time of SC144. Furthermore, the cytotoxicity of SC144 in these cell lines seems to be independent of HR, p53, pRb, p21, HER-2 and p16 status but a careful study is required to provide direct evidence to support this prediction (Table 1). For example, SC144 was equally potent in parental LNCaP and LNCaP HER-2-overexpressing clone, suggesting that its activity is independent of HER-2 expression. It is noteworthy that SC144 showed an excellent activity in HEY cells (IC_{50} = 1.0 ± 0.06 μM) considering that this cell line is resistant to cisplatin, the most commonly used drug in ovarian cancer. The cytotoxicity of SC144 is also prominent in human lung adenocarcinoma cells, CRL5908 and H1299, with IC_{50} values of 3.5 ± 0.3 and 1.67 ± 0.05 μM, respectively. In HR positive (MCF-7 and MDA-MB-468) and negative (MDA-MB-435) human breast cancer cells, SC144 exhibited a good activity. Interestingly, ER-positive cells exhibited a 5.5-fold (MDA-MB-468, IC_{50} = 0.7 ± 0.1 μM) and 2.3-fold (MCF-7, IC_{50} = 1.7 ± 0.3 μM) higher sensitivity to SC144 than ER-negative cell line (MDA-MB-435, IC_{50} = 4.0 ± 0.1 μM) (Table 1). Furthermore, SC144 showed excellent activity against paclitaxel/doxorubicin-resistant NCI/ADR-RES cells, which overexpress multi-drug resistance transporters and P-glycoproteins. Finally, SC144 showed excellent activity in both oxaliplatin-sensitive (HT29) and -resistant (HTOXAR3) colorectal cancer cells with IC_{50} values less than 1 μM. Considering its activity in drug-resistant ovarian cancer NCI/ADR-RES and HEY cells as well as oxaliplatin-resistant colorectal HTOXAR3 cells, SC144 demonstrated promising therapeutic potentials for treatment of human cancers that are refractory to current treatment regimes.

SC144 disrupts cell cycle progression. Cell cycle perturbations induced by SC144 were examined in asynchronous breast cancer MDA-MB-435 cells and colorectal cancer HT29 cells. The analysis of DNA profiles by flow cytometry indicated that SC144 induced cell cycle arrest in G_0/G_1-phase in both cell lines (Fig. 2). Specifically, at 48 h, there was an increase of 16% and 13% of cells retained at G_0/G_1-phase in MDA-MB-435 and HT29 cells, respectively, compared to the corresponding untreated control cells. In a time course experiment, the maximum arrest in HT29 cells was observed 24 h after SC144 exposure. It is worth to mention that at higher cell seeding densities under the same treatment conditions, SC144 causes S-phase accumulation in a comparable manner to CPT-11 (data not shown), suggesting a possible concentration-dependent mechanism for its action. The property of SC144 to induce cell cycle arrest has made it an ideal agent for combination chemotherapy with agents acting at different stages of cell cycle, such as taxanes.

SC144 induces apoptosis. SC144-induced apoptosis was measured by flow cytometry. At its IC_{50}, SC144 caused 15% apoptosis in MDA-MB-435 cells as indicated by sub-G_0/G_1 population (Fig. 3A). An early event in apoptotic cell death is the translocation of

Table 1 **Cytotoxicity of SC144 in various cancer cell lines**

Cell line	Origin	[b]HR	p53	pRb	p16	p21	IC_{50} (μM)[a]
DU-145	Prostate	AR^-	Mut	Null	Mut	Mut	3.0 ± 0.3
LNCaP	Prostate	AR^+	Wt	Wt	Wt	Wt	0.39 ± 0.06
LCCaP/Her2	Prostate	AR^+	Wt	Wt	Wt	Wt	0.4 ± 0.06
HEY	Ovarian	AR^+	Wt	ND	Wt	ND	1.0 ± 0.1
CRL5908	Lung	ND	ND	ND	ND	ND	3.5 ± 0.7
H1299	Lung	$EGFR^+$	Null	Wt	ND	ND	1.67 ± 0.05
CRL5908	Lung	ND	ND	ND	ND	ND	3.5 ± 0.7
MDA-MB-435	Breast	ER^-	Mut	Wt	Wt	Wt	4.0 ± 0.1
MDA-MB-468	Breast	ER^-	Mut	Null	ND	Wt	0.7 ± 0.1
SKBR-3	Breast	ND	ND	ND	ND	ND	3.6 ± 0.5
MCF-7	Breast	ER^+	Wt	Wt	Wt	Wt	1.7 ± 0.3
NCI/ADR-RES	Ovarian	ER^-	Mut	Wt	ND	Wt	0.14
HCT116 $p53^{+/+}$	Colorectal	ND	Wt	Wt	ND	ND	0.58 ± 0.07
HCT116 $p53^{-/-}$	Colorectal	ND	Null	Wt	ND	ND	0.94 ± 0.04
HT29	Colorectal	ND	Mut	Wt	ND	Null	0.9 ± 0.06
HTOXAR3	Colorectal	ND	Mut	ND	ND	Null	0.5 ± 0.1

[a]IC_{50} is defined as drug concentration causing a 50% decrease in cell population. [b]HR, hormone receptor; AR, androgen receptor; ER, estrogen receptor; Wt, wild-type; Mut, mutant; ND, not-determined.

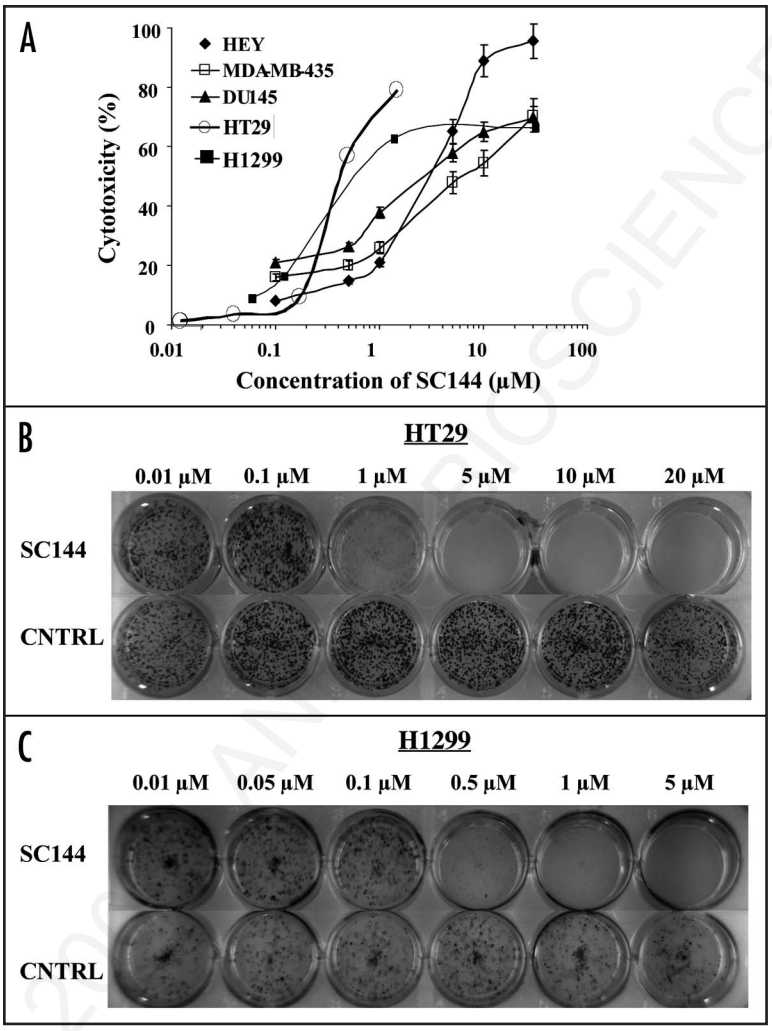

Figure 1. Cytotoxicity of SC144 in representative ovarian, breast, prostate, NSCLC and colon cancer cell lines. (A) The cytotoxicity of SC144 was evaluated in a number of cancer cell lines using MTT assay. (B) Two representative colony formation assays in HT29 and H1299 cells are shown.

the phosphatidyl-serine residues to the outer part of the cell membrane. This event precedes nuclear breakdown, DNA fragmentation and the appearance of most of the apoptosis-associated molecules and is readily measured by annexin V binding assay. By using this method, we measured the percentage of early and late apoptotic cells in HEY cells treated with SC144. As shown in Figure 3B, SC144 triggered early apoptosis and the percentage of early-apoptotic cells increased to 37% at 48 h. A 16% increase in late-apoptosis/necrosis was also observed for SC144 at 48 h.

SC144 moderately inhibits cytochrome P450. The investigation of cytochrome P450 enzyme inhibition by potential drug candidates can aid in predicting drug-drug interactions and/or unfavorable pharmacokinetics profiles produced upon dosing. Competitive inhibition of drug metabolism mediated by important cytochrome P450 enzymes may result in undesirable elevations in plasma drug concentrations, which is of clinical importance for both therapeutic and toxicological reasons. To determine if SC144 inhibits human cytochrome P450 catalytic activity, we performed an in vitro assay specific for CYP3A4 and compared its inhibitory activity with ketoconazole, a well-known substrate as a positive control. As shown in Figure 4, SC21, an analogue of SC144, did not significantly inhibit CYP3A4 activity, while SC144 exhibited moderate CYP3A4 inhibitory activity at its IC_{50} even though it possesses favorable calculated ADMET properties. It is important to bear in mind that many drugs including anticancer agents undergo CYP450-mediated hepatic metabolism before excretion. Understanding this activity is critical for

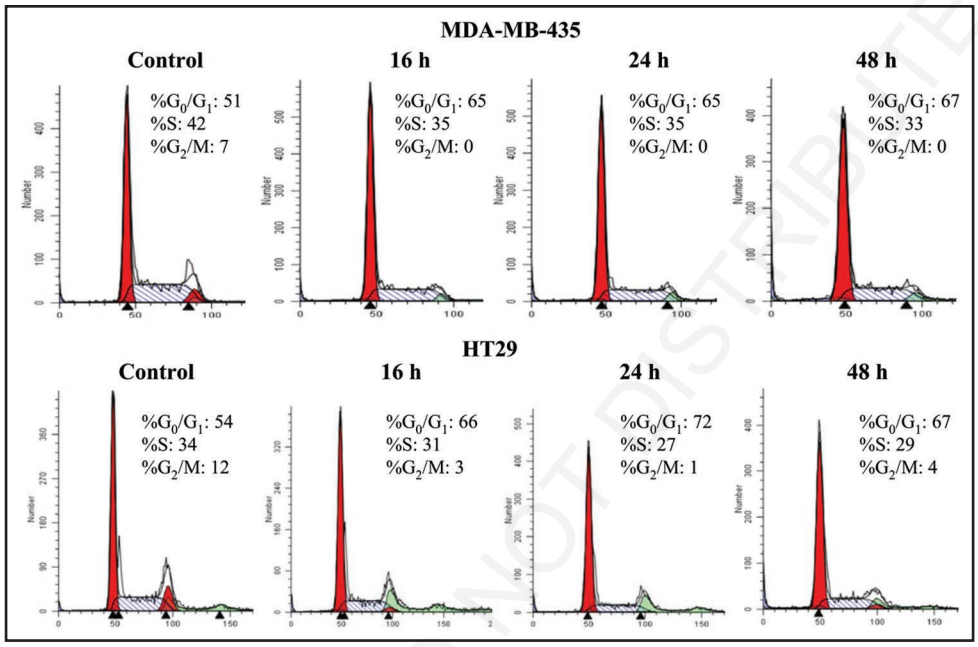

Figure 2. Flow cytometry analysis of the cell cycle profiles of MDA-MB-435 and HT29 cells treated with SC144. Cells were treated for 16 h, 24 h and 48 h with SC144, stained with PI and analyzed for their effect on the cell cycle.

individualized cancer therapy,[13,14] since many anticancer drugs inhibit CYP3A4 in low micromolar concentrations (reviewed in ref. 15). Because of its moderate inhibition on P450 activity, the toxicity and tolerance of SC144 will be monitored carefully in our future in vivo studies. Detailed kinetics studies are under way to understand the pharmacokinetics profiles of SC144.

SC144 shows in vivo efficacy in mice xenograft models. The in vivo efficacy of SC144 was first evaluated in nude mice xenograft model of human breast cancer MDA-MB-435. A schematic outline of the experimental procedure is shown in Figure 5A. Animals were treated with daily I.P. injections of sesame oil (controls) or SC144 at 0.3 mg/kg, 0.8 mg/kg and 4 mg/kg. After fifteen-days of dosing, the drug treatment was discontinued and the animals were monitored biweekly for five weeks. Figure 5B shows the volume (mean ± SD) of SC144-treated MDA-MB-435 xenografts over time. For statistical analysis, the %T/C value was calculated on day 31 of dosing and is plotted for all treatment groups (Fig. 5C). A moderate but significant reduction was observed at the lowest dose in breast cancer xenografts ($p < 0.05$ at day 31). Significant reduction in tumor growth was observed at higher doses and SC144 inhibited tumor growth by 60% at 4 mg/Kg ($p < 0.001$). A representative image of mice with and without SC144 treatment at the end of the study is shown in Figure 5D. Compared to control tumors, SC144-treated tumors were markedly smaller in size, less vascularized and remained localized (Fig. 5E).

The in vivo efficacy of SC144 was also evaluated in human colon cancer HT29 xenograft models. Unfortunately, SC144 is practically insoluble in numerous formulations we tried. To increase the solubility of SC144, various salts were prepared and HCl salt was selected for this particular study. Animals were therefore treated with daily I.P. injections of sesame oil (controls) or HCl salt of SC144 at 10 mg/kg, 25 mg/kg, 50 mg/kg, 100 mg/kg, 125 mg/kg and 150 mg/kg. Similar to the findings in MDA-MB-435 xenograft model using SC144 in a base form, SC144.HCl was able to inhibit the tumor growth at doses above 25 mg/kg in in vivo colorectal cancer HT29 model (Fig. 6). However, at the end of the experiments we observed a significant amount of drug had precipitated and formed a white film. This lack of drug absorption is perhaps responsible for the lower efficacy of SC144.HCl in HT29 xenograft model. Under these conditions the treatment with SC144 was well tolerated in HT29 xenograft model and did not result in any body weight loss (data not shown) or drug-related deaths even at doses of 150 mg/kg.

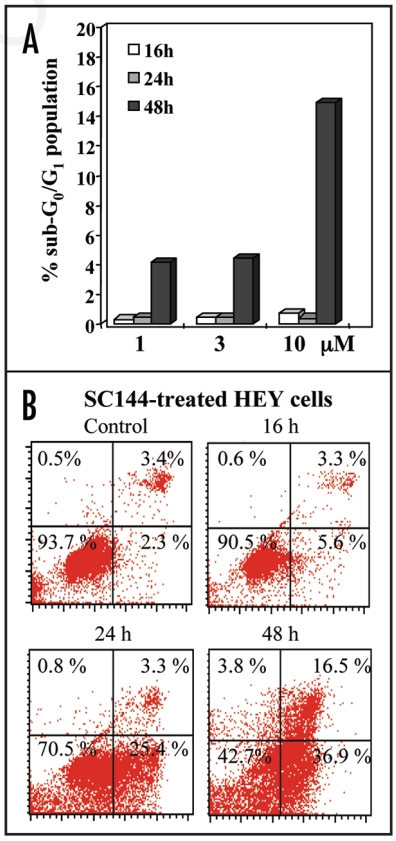

Figure 3. SC144 triggers apoptosis in select cancer cell lines. (A) Percentage of apoptosis induced by SC144 in MDA-MB-435 cells was calculated by measuring sub-G_0/G_1 population using flow cytometry. Apoptotic population increased with time, reaching to 15% in SC144 treated cells. Percent errors were between 2–7%. (B) Apoptosis analysis of HEY cells treated with SC144 (IC_{80}). Cells were stained with annexin V/propidium iodide and analyzed by flow cytometry. Cells in the bottom left quadrant of each panel (Annexin V-negative, propidium iodide-negative) are viable, whereas cells in the bottom right quadrant (Annexin V-positive, propidium iodide-negative) are in the early stages of apoptosis, and cells in the top right quadrant (Annexin V-positive, propidium iodide-positive) are in later stages of apoptosis and necrosis.

Discussion

The need to develop novel drugs with better efficacy and safety profiles is pressing. Herein, we synthesized a series of analogues of previously reported SC21 and SC23. Among these analogues, SC144,

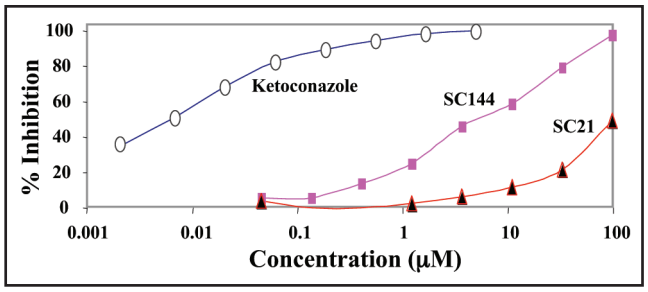

Figure 4. Inhibition of human CYP3A4 by ketoconazole, SC144, and SC21 in MDA-MB-435 cells. The metabolism of fluorescent substrates by human cDNA-expressed CYP3A4 was assessed by incubation in a 96-well plate at 37°C. Metabolism of 7-benzyloxy-4-trifluoromethylcoumarin was assayed by measuring the production of the corresponding 7-hydroxy-4-trifluoro-methyl coumarin.

which exhibits favorable physicochemical properties as predicted by ADMET calculation software, was selected for further evaluation on its efficacy against a panel of human tumor-derived cancer cell lines. SC144 inhibited cancer cell growth in a time- and dose-dependent manner in several hormone-dependent and -independent tumor cells, suggesting its potential for the treatment of hormone receptor-positive and -negative cancers. It is now widely appreciated that a major obstacle in combating cancers is the acquired resistance by cancer cells after exposure to chemotherapeutic agents.[16] As a lead anticancer agent, the broad therapeutic potential of SC144 was further underscored by its potency in drug-resistant cancer cells, including NCI/ADR-RES, HEY and HTOXAR3 cells, demonstrated in the current study. Recently, we explored the combination effect of SC144 with select cytotoxic anticancer agents and found that SC144 elicits synergism with 5-flurouracil, oxaliplatin and paclitaxel in relevant cancer settings,[17] pointing out a promising future direction for its clinical development in combination therapy.

Consistent with its effects on cell growth inhibition, we also demonstrated that SC144 disrupted cell cycle progression and induced apoptosis in select cancer cells. It is known that most anticancer drugs induce apoptosis.[18] Considering the profound effect of apoptosis on cancer progression and response to chemotherapy, reactivating apoptotic pathway appears to be an attractive strategy for anticancer drug therapy.[19-22] Based on annexin V/propidium iodide staining and sub-G_0/G_1 fractions, we concluded that SC144 elicited its cytotoxicity, at least in part, through apoptosis signaling. The potent in vitro efficacy of SC144 was also confirmed by its in vivo antitumor activity in both MDA-MB-435 and HT29 mice xenograft models, further suggesting its potential application as a novel anticancer agent.

A number of characteristics of SC144 indicate that this compound has promising potentials as possible anticancer chemotherapeutics. As a small-molecule compound, SC144 is stable under physiological conditions and readily crosses cell membranes, which provides a clear advantage over peptide or oligonucleotide agents that typically require significant modifications to enhance stability and cell-permeability. Furthermore, SC144 possesses the essential drug-like properties, in contrast to many lead compounds that need significant chemical modifications to obtain desirable physicochemical properties. In addition to these favorable properties, the simple and straightforward synthesis of SC144 also makes it more advantageous over compounds that can only be prepared in low yield due to multiple synthetic steps.

In conclusion, our preclinical evaluation suggests that SC144 represents a novel class of anticancer drugs. As a prototype of quinoxalinehydrazides, SC144 demonstrates significant in vitro and in vivo activity and its potency in a number of drug-resistant cancer cell lines makes it an attractive agent for further development. We recently carried out a lead optimization based on a structure-activity relationship study and discovered SC161 with better potency in cancer cell lines.[23] The future perspective of this work is to discern the mechanisms of the anticancer activity of SC144 by DNA microarray and proteomics analysis. The results of these studies will be reported in due course.

Materials and Methods

Chemistry. All reactions were carried out under a nitrogen atmosphere. Progress of the reaction was monitored by thin layer chromatography on silica gel plates (Merck 60, F_{254}, 0.2 mm). Melting points were measured using a Gallenkamp apparatus and are uncorrected. IR spectra were recorded as thin films on Perkin-Elmer 398 and FT 1600 spectrophotometers. ^{1}H NMR spectra were recorded on a Brüker 300-MHz spectrometer with TMS as an internal standard: chemical shifts are expressed in d values (ppm) and coupling constants (*J*) in Hz. Mass spectral data were determined by direct insertion at 70 eV with a VG70 spectrometer. Merck silica gel (Kieselgel 60/230–400 mesh) was used for flash chromatography columns. Elemental analyses were performed on a Perkin-Elmer 240C elemental analyzer, and the results were within ± 0.4% of the theoretical values.

Synthesis of 4-chloro-7-fluoropyrrolo[1,2-*a*]quinoxaline (5). A mixture of 7-fluoro-5*H*-pyrrolo[1,2-*a*]quinoxalin-4-one (101 mg, 0.5 mmol) prepared as previously described[12] and phosphoryl chloride (0.46 mL, 5 mmol) was refluxed for 4 h under nitrogen. After cooling, the mixture was poured into crushed ice and extracted with dichloromethane. The organic layer was washed with brine, dried and evaporated. The residue obtained was purified by flash-chromatography (ethyl acetate) to give the title compound as colorless prisms (100 mg, 90% yield); (cyclohexane); mp 193°C; ^{1}H NMR ($CDCl_3$) 6.86 (m, 1 H), 7.03 (m, 1 H), 7.25 (m, 1 H), 7.56 (dd, 1 H, *J* = 8.8, 2.9 Hz), 7.76 (m, 1 H), 7.90 (d, 1 H, *J* = 3.3 Hz). MS (CI) *m/z* 221 (MH^+). Anal. Calcd for $C_{11}H_6ClFN_2$: C, H, N.

Synthesis of 7-fluoro-4-hydrazinopyrrolo[1,2-*a*]quinoxaline (6). A mixture of 7-fluoro-4-chloropyrrolo[1,2-*a*]quinoxaline 5 (100 mg, 0.45 mmol) and hydrazine monohydrate (5 mL) in DMF (2 mL) was heated at 70–80°C for 1 h. Crushed ice was then added and the mixture was extracted with ethyl acetate. The organic layer was separated and shaken with water and brine successively. After evaporation of the solvents, compound **6** was obtained as a solid (84 mg, 86% yield) and used in the subsequent step without further purification. An analytical sample was obtained by crystallization; (dichloromethane/light petroleum); mp 158°C (dec.); IR (KBr) 3,300 cm^{-1}; ^{1}H NMR (DMSO-d_6) 4.56 (bs, 2 H), 6.66 (t, 1 H, *J* = 3.2 Hz), 7.03 (m, 2 H), 7.18 (dd, 1 H, *J* = 10.6, 2.7 Hz), 8.02 (dd, 1 H, *J* = 8.9, 5.6 Hz), 8.15 (s, 1 H), 8.87 (bs, 1 H). Anal. Calcd. for $C_{11}H_9FN_4$: C, H, N.

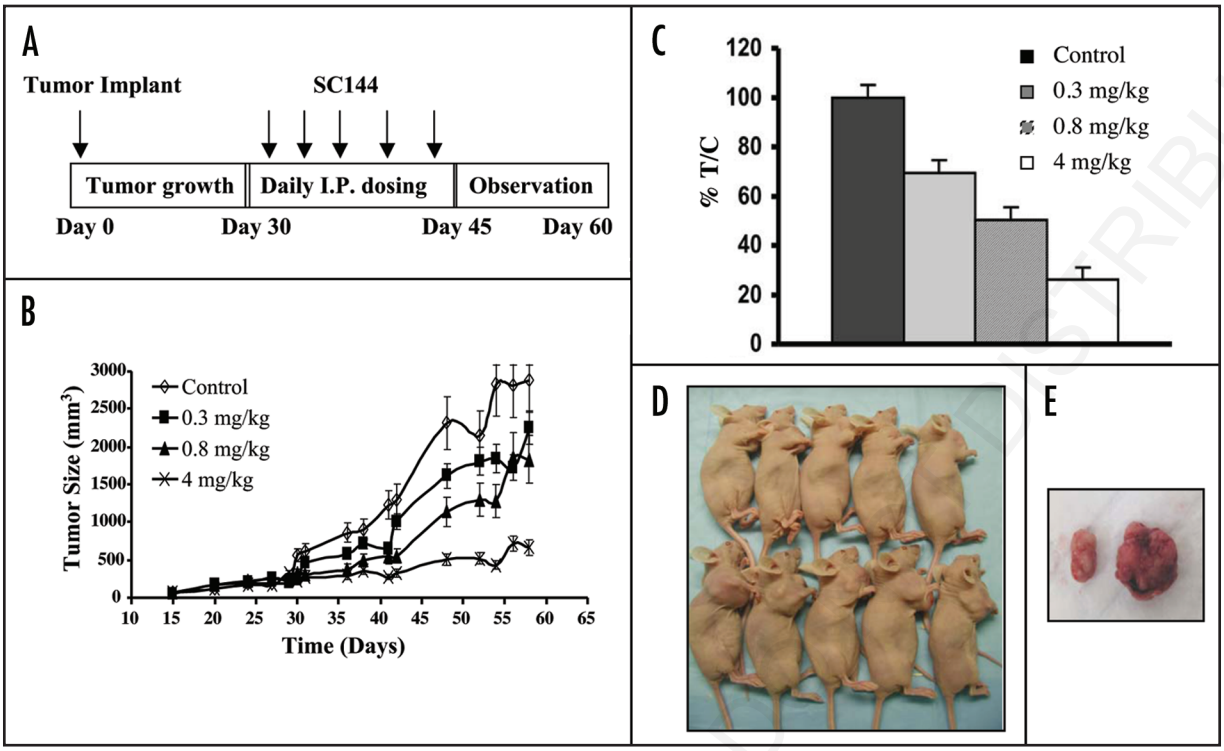

Figure 5. In vivo efficacy of SC144 in MDA-MB-435 xenograft model. (A) Schematic outline of tumor growth and dosing in breast cancer xenograft model. Athymic nude mice (n = 10) implanted with MDA-MB-435 cells were treated with the indicated doses of SC144 by daily I.P. administration for 15 days. (B) SC144 reduced the sizes of tumors all doses tested. Values represent the median tumor weight for each group. (C) The %T/C for each treatment group was calculated on day 31 of the experiment (Mean ± SD). (D) A representative comparison image of the control and SC144-treated mice. (E) A representative image of the incised control and treated tumor.

Synthesis of *N*'-(7-fluoropyrrolo[1,2-*a*]quinoxalin-4-yl) pyrazine-2-carbohydrazide (SC144). To a stirred suspension of 2-pyrazinecarboxylic acid (62 mg, 0.50 mmol) in dry, dichloromethane (2 mL) were added portion-wise within 1 h, triphenylphosphine (262 mg, 1.00 mmol) and 2,2'-dipyridyl disulfide (220 mg, 1.00 mmol). When the starting material disappeared, a solution of 7-fluoro-4-hydrazinopyrrolo[1,2-*a*] quinoxaline (108 mg, 0.50 mmol) in the same solvent (6 mL) was added and the resulting mixture was stirred at room temperature overnight. The solvent was removed and the residue was partitioned between ethyl acetate and water. The organic layer was separated, shaken with brine and dried over $MgSO_4$. The resulting residue was purified by flash-chromatography (chloroform:methanol:ammonium hydroxide, 89:10:1) to afford SC144 as a pale yellow solid (56 mg, 35% yield); (methanol/ethyl acetate); mp 195°C (dec.); IR (KBr) 3255, 1,690 cm^{-1}; ^1H NMR (DMSO-d_6) 3.75 (bs, 1 H), 6.96 (m, 1 H), 7.35 (t, 1 H, J = 8.7 Hz), 7.68 (m, 2 H), 8.30 (dd, 1 H, J = 8.7, 4.8 Hz), 8.60 (s, 1 H), 8.82 (m, 1 H), 8.94 (d, 1 H, J = 2.7 Hz), 9.22 (s, 1 H), 11.67 (bs, 1 H). MS (MALDI, TOF/TOF) *m/z* 323.0983 (MH^+) requires 323.1056. Anal. Calcd. for $C_{16}H_{11}FN_6O$: C, H, N.

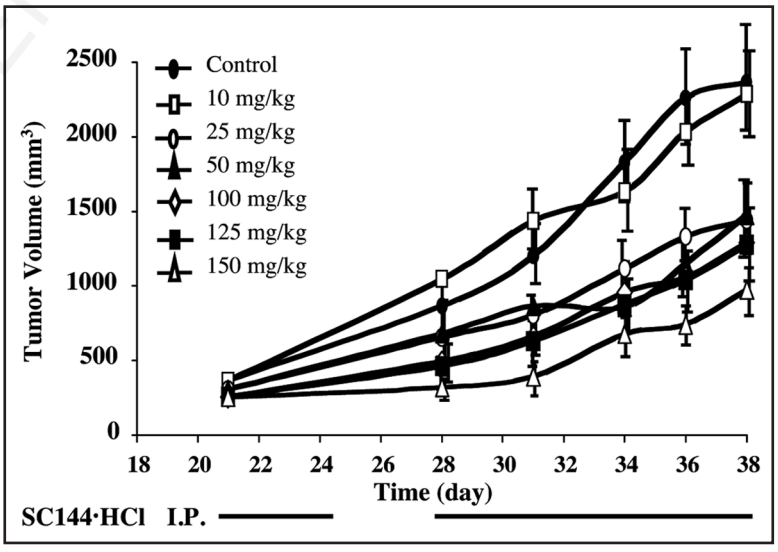

Figure 6. In vivo efficacy of SC144 in HT29 xenograft model. SC144.HCl inhibited the growth of tumors at doses above 25 mg/Kg in colon cancer mice xenograft model.

Cell culture. Human prostate cancer cells (PC-3: $p53^{-/-}$, AR^-; DU-145: p53 mutant, AR^-; and LNCaP: p53 wild-type, AR^+), breast cancer cells (MCF-7: overexpressed wild-type p53, ER^+; MDA-MB-468: p53 mutant, ER^+; and MDA-MB-435: p53 mutant, ER^-), non-small cell lung cancer cells H1299 ($p53^{-/-}$, $EGFR^+$) were purchased from the American Type Cell Culture (Manassas, VA). Human ovarian carcinoma cell line (HEY) naturally resistant to cisplatin (CDDP) was kindly provided by Dr. Louis Dubeau (USC Norris Cancer Center).[24,25] SKBR-3 cells were kindly provided by Dr. Alan Epstein (USC, Department of Pathology). HTOXAR3 cells were generated by growing HT-29 cells in the presence of oxaliplatin for a year as described previously.[26] The LNCaP/HER-2 cells were a gift from Dr. Richard Cote (USC, Department of Pathology).

HCT116 $p53^{+/+}$ and HCT116 $p53^{-/-}$ cells were kindly provided by Dr. Bert Vogelstein (Johns Hopkins Medical Institutions, Baltimore, MD). Cells were maintained as monolayer cultures in the appropriate media: RPMI 1640, McCoy's 5A (SKBR-3) or DMEM (MDA-MB-435 and MDA-MB-468) supplemented with 10% fetal bovine serum (FBS) (Gemini-Bioproducts, Woodland, CA) and 2 mmol/L L-Glutamine at 37°C in a humidified atmosphere of 5% CO_2. To remove the adherent cells from the flask for subculture and counting, cells were washed with PBS without calcium or magnesium, incubated in a small volume of 0.25% trypsin-EDTA solution (Sigma-Aldrich, St. Louis, MO) for 5 min, resuspended with culture medium and centrifuged at 1,200 rpm for 5 min. All experiments were performed using cells in exponential growth phase. Cells were routinely checked for *Mycoplasma* contamination using PlasmoTest (InvivoGen, San Diego, CA).

Drug dilutions. 10 mM stock solutions of all compounds were prepared in DMSO and stored at -20°C. Further dilutions were freshly made in PBS or cell-culture media.

Cytotoxicity assays. Cytotoxicity was assessed by 3-(4,5-dimethylthiazol-2-yl)-2,5-diphenyltetrazolium bromide (MTT) assay as previously described.[27] Briefly, cells were seeded in 96-well microtiter plates and allowed to attach overnight. Cells were subsequently treated with continuous exposure to corresponding drugs for 72 h. An MTT solution (at a final concentration of 0.5 mg/mL) was added to each well and cells were incubated for 4 h at 37°C. After removal of the supernatant, DMSO was added and the absorbance was read at 570 nm. All assays were done in triplicate. The IC_{50} was then determined for each drug from a plot of log (drug concentration) versus percentage of cell killed.

Cell cycle analysis. Cell cycle perturbation was analyzed by propidium iodide (PI) DNA staining. Briefly, exponentially growing cells (MDA-MB-435 and HT29) were treated with corresponding IC_{50} doses of SC144 for various times. At the end of each treatment, cells were collected and washed with PBS followed by a gentle centrifugation at 1,200 x*g* for 5 min. Cells were thoroughly resuspended in 0.5 mL of PBS and fixed in 70% ethanol overnight at -20°C. Ethanol-resuspended cells were then centrifuged at 1,200 x*g* for 5 min and washed twice in PBS to remove residual ethanol. For cell cycle analysis, the pellets were resuspended in 1 mL of PBS containing 0.02 mg/mL of propidium iodide and 0.5 mg/mL of DNase-free RNase A and incubated at room temperature for 30 min. Cell cycle profiles were obtained using a BD LSRII flow cytometer (BD Biosciences, San Jose, CA) and data were analyzed by ModFit LT software (Verity Software House, Inc., Topsham, ME).

Apoptosis assay. To quantify drug-induced apoptosis, cells were stained with annexin V/propidium iodide and counted by flow cytometry. Briefly, after drug treatments (IC_{80} of each drug for up to 48 h), both floating and attached cells were collected and subjected to annexin V/propidium iodide staining using annexin V-FITC apoptosis detection kit (Oncogene Research Products, San Diego, CA) according to manufacturer's recommendation. Untreated cells (24 and 48 h) were maintained in parallel with the treated group. In cells undergoing apoptosis, annexin V binds to phosphatidylserine, which is then translocated from the inner to the outer leaflet of the cytoplasmic membrane. Double staining is used to distinguish between viable, early apoptotic and necrotic or late apoptotic cells.[28] The resulting fluorescence (FLH-1 channel for green fluorescence and FLH-2 channel for red fluorescence) was measured by flow cytometry using a FACScan flow cytometer (Becton Dickinson, San Jose, CA). According to this method, the lower left quadrant shows the viable cells, the upper left quadrant shows cell debris, the lower right quadrant shows the early apoptotic cells, and the upper right quadrant shows the late apoptotic and necrotic cells.

Inhibition of cytochrome P450 CYP3A4. The inhibitory effect of SC144 on cytochrome P450 was examined by measuring the metabolism of fluorescent substrates mediated by human cDNA-expressed CYP3A4. Incubation was performed in a 96-well plate format at 37°C, using 7-benzyloxy-4-trifluoromethylcoumarin as fluorescent substrates. Metabolism of the model substrate was assayed by measuring the production of the corresponding 3-[2-(N,N-diethylamino)ethyl]-7-hydroxy-4-methyl coumarin metabolite, which was detected by fluorescence using a microplate reader.

Animals. 100 female virgin athymic nude (*nu/nu*) mice (Charles River Laboratories, Wilmington, MA) were used for in vivo efficacy testing with 2 select cell lines. The animals were fed *ad libitum* and kept in air-conditioned rooms at 20 ± 2°C with a 12 h light-dark period. Animal care and manipulation were in agreement with the USC institutional guidelines, which were in accordance with the Guidelines for the Care and Use of Laboratory Animals.

In Vivo mice xenograft studies. Human breast cancer MDA-MB-435 cells in logarithmic growth phase from in vitro cell culture were inoculated subcutaneously in the flank of athymic nude mice (2 x 10^6 cells/mouse) under aseptic conditions. Tumor growth was assessed by biweekly measurement of tumor diameters with a Vernier caliper (length x width). Tumor weight was calculated according to the formula: TW (mg) = tumor volume (mm^3) = d^2 x $D/2$, where d and D are the shortest and longest diameters, respectively. Tumors were allowed to grow to an average volume of 100 mm^3. Animals were then randomly assigned as control and treatment groups, to receive control vehicle or SC144 (0.3, 0.8 and 4 mg/kg, dissolved in sesame oil) via I.P. injections once a day for 15 days. Treatment of each animal was based on individual body weight. After treatment, tumor volumes in each group were measured once a week for 4 weeks. The percentage of tumor growth inhibition was calculated as T/C% = 100 x (mean TW of treated group)/(mean TW of control group).

Human colon cancer HT-29 cells in logarithmic growth phase were inoculated subcutaneously in the flank of athymic nude mice (5 x 10^6 cells/mouse) under aseptic conditions. Tumor growth was assessed and monitored as described above. When tumor sizes reached an average volume of 300 mm^3, animals were randomly assigned to control and treatment groups to received control vehicle or SC144. HCl (10, 25, 50, 100, 125 and 150 mg/kg) via I.P. injection for 15 days. The tumor volumes in each group were measured once a week until the control tumor reached 2,000 mm^3. Treated animals were checked daily for treatment-related toxicity/mortality.

Statistical analysis. In vitro assays were set up in triplicates and the results were expressed as means ± SD. Statistical analysis and p-value determination were done by two-tailed paired t test with a confidence interval of 95% for determination of the significant differences between treatment groups. $p < 0.05$ was considered to

be statistically significant. ANOVA was used to test for significance among groups. The SAS statistical software package (SAS Institute, Cary, NC) was used for statistical analysis.

Acknowledgements

This work was supported by grants from the Department of Defense OCRP Idea Award, Jeannik M. Littlefield-AACR, and the Wittier Foundation to N.N. and "Fondazione Carical, Cosenza, Italy" to F.G. We would like to thank Osvaldo De Grazia, Marie Martinez, Lisa Yan and Leah Movesseisia for their technical assistance.

References

1. Neamati N, Barchi JJ Jr. New paradigms in drug design and discovery. Curr Topics Med Chem 2002; 2:211-27.
2. Cattley RC, Radinsky RR. Cancer therapeutics: understanding the mechanism of action. Toxicol Pathol 2004; 32:116-21.
3. Wang J, Ramnarayan K. Toward designing drug-like libraries: a novel computational approach for prediction of drug feasibility of compounds. J Comb Chem 1999; 1:524-33.
4. Netzer R, Ebneth A, Bischoff U, Pongs O. Screening lead compounds for QT interval prolongation. Drug Discov Today 2001; 6:78-84.
5. Lindpaintner K. The impact of pharmacogenetics and pharmacogenomics on drug discovery. Nature Rev 2002; 1:463-9.
6. Fermini B, Fossa AA. The impact of drug-induced QT interval prolongation on drug discovery and development. Nature Rev 2003; 2:439-47.
7. McLeod HL, Yu J. Cancer pharmacogenomics: SNPs, chips and the individual patient. Cancer Invest 2003; 21:630-40.
8. Di Paolo A, Danesi R, Del Tacca M. Pharmacogenetics of neoplastic diseases: new trends. Pharmacol Res 2004; 49:331-42.
9. Zhu F, Zheng CJ, Han LY, Xie B, Jia J, Liu X, Tammi MT, Yang SY, Wei YQ, Chen YZ. Trends in the exploration of anticancer targets and stategies in enhancing the efficacy of drug targeting. Curr Mol Pharmacol 2008; 1:213-32.
10. Plasencia C, Dayam R, Wang Q, Pinski J, Burke TR Jr, Quinn DI, Neamati N. Discovery and preclinical evaluation of a novel class of small-molecule compounds in hormone-dependent and -independent cancer cell lines. Mol Cancer Ther 2005; 4:1105-13.
11. Grande F, Aiello F, Grazia OD, Brizzi A, Garofalo A, Neamati N. Synthesis and antitumor activities of a series of novel quinoxalinhydrazides. Bioorg Med Chem 2007; 15:288-94.
12. Campiani G, Cappelli A, Nacci V, Anzini M, Vomero S, Hamon M, Cagnotto A, Fracasso C, Uboldi C, Caccia S, Consolo S, Mennini T. Novel and highly potent 5-HT3 receptor agonists based on a pyrroloquinoxaline structure. J Med Chem 1997; 40:3670-8.
13. Fujita K. Cytochrome P450 and anticancer drugs. Curr Drug Meta 2006; 7:23-37.
14. Rodriguez-Antona C, Ingelman-Sundberg M. Cytochrome P450 pharmacogenetics and cancer. Oncogene 2006; 25:1679-91.
15. Sanchez RI, Mesia-Vela S, Kauffman FC. Challenges of cancer drug design: a drug metabolism perspective. Curr Cancer Drug Targets 2001; 1:1-32.
16. Hanahan D, Weinberg RA. The hallmarks of cancer. Cell 2000; 100:57-70.
17. Oshima T, Cao X, Grande F, Yamada R, Garofalo A, Louie S, Neamati N. Combination effects of SC144 and cytotoxic anti-cancer agents. Anti-Cancer Drugs 2009; (in press).
18. Lowe SW, Lin AW. Apoptosis in cancer. Carcinogenesis 2000; 21:485-95.
19. Assuncao Guimaraes C, Linden R. Programmed cell deaths. Apoptosis and alternative deathstyles. Euro J Biochem/FEBS 2004; 271:1638-50.
20. Norbury CJ, Zhivotovsky B. DNA damage-induced apoptosis. Oncogene 2004; 23:2797-808.
21. Pommier Y, Sordet O, Antony S, Hayward RL, Kohn KW. Apoptosis defects and chemotherapy resistance: molecular interaction maps and networks. Oncogene 2004; 23:2934-49.
22. Sun SY, Hail N Jr, Lotan R. Apoptosis as a novel target for cancer chemoprevention. J Natl Cancer Inst 2004; 96:662-72.
23. Deng J, Taheri L, Grande F, Aiello F, Garofalo A, Neamati N. Discovery of novel anticancer compounds based on a quinoxalinehydrazine pharmacophore. ChemMedChem 2008; 3:1677-86.
24. Buick RN, Pullano R, Trent JM. Comparative properties of five human ovarian adenocarcinoma cell lines. Cancer Res 1985; 45:3668-76.
25. Hamaguchi K, Godwin AK, Yakushiji M, O'Dwyer PJ, Ozols RF, Hamilton TC. Cross-resistance to diverse drugs is associated with primary cisplatin resistance in ovarian cancer cell lines. Cancer Res 1993; 53:5225-32.
26. Plasencia C, Martinez-Balibrea E, Martinez-Cardus A, Quinn DI, Abad A, Neamati N. Expression analysis of genes involved in oxaliplatin response and development of oxaliplatin-resistant HT29 colon cancer cells. Int J Oncol 2006; 29:225-35.
27. Carmichael J, DeGraff WG, Gazdar AF, Minna JD, Mitchell JB. Evaluation of a tetrazolium-based semiautomated colorimetric assay: assessment of chemosensitivity testing. Cancer Res 1987; 47:936-42.
28. Fadok VA, Voelker DR, Campbell PA, Cohen JJ, Bratton DL, Henson PM. Exposure of phosphatidylserine on the surface of apoptotic lymphocytes triggers specific recognition and removal by macrophages. J Immunol 1992; 148:2207-16.